

Regeneration of the Ferrous Heme of Soluble Guanylate Cyclase from the Nitric Oxide Complex: Acceleration by Thiols and Oxyhemoglobin[†]

Philip E. Brandish,[‡] Wolfgang Buechler,[§] and Michael A. Marletta^{*,‡,||,⊥}

Department of Biological Chemistry, University of Michigan Medical School, Howard Hughes Medical Institute and Interdepartmental Program in Medicinal Chemistry, College of Pharmacy, University of Michigan, Ann Arbor, Michigan 48109-1065, and Division of Clinical Pharmacology, Medizinische Klinik Innenstadt, 80336 Munich, Germany

Received June 24, 1998; Revised Manuscript Received October 5, 1998

ABSTRACT: Soluble guanylate cyclase (sGC) catalyzes the conversion of GTP to cGMP and is activated several hundred-fold by binding of nitric oxide (•NO) to the heme prosthetic group. We have examined the stability of the nitrosyl-heme complex of sGC (•NO-sGC) at 37 °C in order to determine whether simple dissociation of •NO from sGC could account for the observed in vivo deactivation time. Recombinant sGC was purified from Sf9 cells coinfecting with baculoviruses containing the cDNAs for the $\alpha 1$ and $\beta 1$ subunits of rat lung sGC. The purified protein contained a stoichiometric equivalent of ferrous high-spin heme. Characterization of the purified protein found it to be essentially identical to that purified from bovine lung. Ferrous-nitrosyl sGC prepared anaerobically and exchanged into aerobic buffer containing no reducing agents was essentially stable on ice and had a half-life of approximately 90 min at 37 °C. In the presence of thiols [DTT, glutathione (GSH), or L-cysteine], •NO was rapidly lost from sGC regenerating the ferrous high-spin form of the heme. The half-life of •NO-sGC in the presence of 1 mM GSH at 37 °C was 6.3 min. In the presence of oxyhemoglobin, the half-life was further reduced to 2.9 min. Although these rates are not fast enough to account for that observed in vivo, and thus probably involve additional agent(s), these data do imply a role for low molecular weight thiols, such as GSH, and oxyferrohemoproteins, such as oxymyoglobin, in the deactivation of sGC.

Soluble guanylate cyclase (sGC, EC 4.6.1.2)¹ catalyzes the conversion of GTP to cGMP and pyrophosphate (1, 2). The protein contains high-spin ferrous heme as isolated from bovine lung and is activated by nitric oxide (•NO) (1, 3–5). sGC mediates the vasorelaxant and neurostimulatory effects

of •NO, produced from L-arginine by nitric oxide synthase (NOS), via elevation of intracellular cGMP (2, 6). This nucleotide cyclase is a member of a family of nucleotide cyclases which include the adenylate cyclases (ACs) and the particulate guanylate cyclases (pGCs). All of these enzymes have catalytic domains which share significant homology (7–9). The difference between them lies in the activation of the catalytic activity: G-proteins and the plant-derived terpenoid forskolin in the case of ACs (10), extracellular hormone signals such as atrial natriuretic factor in the case of the pGCs (7, 11), and •NO in the case of sGC. The ACs are monomeric proteins containing two homologous regions which associate to form a catalytic site (10, 12), the pGCs are homodimeric proteins (9, 13), and sGC is a heterodimeric protein (3, 14, 15). sGC consists of a 79 kDa α -subunit and a 70.5 kDa β -subunit, the cDNA pairs for which have been cloned from rat lung, bovine lung, human brain, *Drosophila*, and the fish *O. latipes* (16–21).

The heme cofactor of sGC has been shown to be ligated by an axial histidine (3). The bond between heme iron and histidine imidazole nitrogen is weak as identified by resonance Raman spectroscopy (22, 23). This property of the heme environment in part accounts for the observation that sGC does not bind oxygen (22, 23). Ferrous hemoproteins which bind oxygen (e.g., Hb and Mb) react with •NO to give ferric heme and nitrate (24, 25). Thus, not binding oxygen allows sGC to function as an •NO-sensor in the presence of oxygen as is the case in vivo. Upon binding of

[†] This work was supported by the Howard Hughes Medical Institute and by a NATO Postdoctoral Fellowship grant (P.E.B.) from the Royal Society, England. This work was done in part during the tenure of a Research Fellowship (P.E.B.) of the American Heart Association, Michigan Affiliate.

* To whom correspondence should be addressed at 5315 Medical Sciences, University of Michigan Medical School, Ann Arbor, MI 48109-0606.

[‡] Interdepartmental Program in Medicinal Chemistry, University of Michigan.

[§] Division of Clinical Pharmacology, Medizinische Klinik Innenstadt.

^{||} Department of Biological Chemistry, University of Michigan Medical School.

[⊥] Howard Hughes Medical Institute, University of Michigan.

¹ Abbreviations: AC, adenylate cyclase; BSA, bovine serum albumin; CAPS, 3-(cyclohexylamino)-1-propanesulfonic acid; CO, carbon monoxide; cGMP, guanosine 3',5'-cyclic monophosphate; DTT, dithiothreitol; EDTA, ethylenediaminetetraacetic acid; GSH, reduced glutathione; GSNO, S-nitrosoglutathione; GSSG, oxidized glutathione; GTP, guanosine 5'-triphosphate; Hb, hemoglobin; IBMX, isobutylmethylxanthine; Mb, myoglobin; MOI, multiplicity of infection; MOPS, 3-(N-morpholino)propanesulfonic acid; •NO, nitric oxide; NOS, nitric oxide synthase; pGC, particulate guanylate cyclase; PMSF, phenylmethylsulfonyl fluoride; PVDF, poly(vinylidene difluoride); sGC, soluble guanylate cyclase; SDS-PAGE, sodium dodecyl sulfate-polyacrylamide gel electrophoresis; SNP, sodium nitroprusside; TEA, triethanolamine; TFA, trifluoroacetic acid; YC-1, 3-(5'-hydroxymethyl-2'-furyl)-1-benzylindazole.

•NO, the iron–histidine bond is broken, and a five-coordinate ferrous-nitrosyl species is formed, concomitant with activation of catalysis (4, 26, 27). Carbon monoxide (CO) or the synthetic benzylindazole derivative, YC-1, has also been shown to activate sGC, although neither of them to the same degree as •NO (3, 28–30). CO binds to the heme of sGC to form a six-coordinate complex (3). The bond between the axial histidine and the heme iron is not broken as when •NO binds. This may be related to the fact that activation by CO is low compared to that by •NO. The effect of YC-1 is synergistic with that of CO, together activating sGC to the same level as with •NO, but the mechanism of activation is unknown (29, 31). The activation of sGC by YC-1 might be analogous to activation of AC by forskolin. Forskolin binds to the catalytic portion of AC (12, 32).

Experiments performed with a bioassay using sections of rabbit aorta connected to a column of cultured endothelial cells showed that, after relaxation induced by •NO (EDRF) that was released by the endothelial cells upon treatment with bradykinin, tissue recontracted to its original state within 1–2 min (33). The same preparation could be restimulated with •NO immediately after the first stimulus. Thus, deactivation of sGC in vivo is rapid, probably with a half-life of less than 1 min. The dissociation of •NO from typical nitrosyl complexes of hemoproteins such as myoglobin and T- and R-state hemoglobin is variable, with rate constants ranging from 1×10^{-3} to $1.8 \times 10^{-5} \text{ s}^{-1}$ at 20 °C (34–36). The rate of dissociation of •NO from 5-coordinate Fe^{II} –porphyrin–NO model compounds in toluene at 25 °C varied from 4.2×10^{-5} to 47.1 s^{-1} depending on the porphyrin structure and the competing ligand (37). Kharitonov et al. measured a dissociation rate constant of $6 \times 10^{-4} \text{ s}^{-1}$ at 20 °C for •NO-sGC (36). Subsequently the same investigators found that substrate (MgGTP) increased the rate of dissociation by approximately 70-fold (38). Dierks and Burstyn contended that a redox reaction of the heme-nitrosyl adduct may be a mechanism for deactivation, since sGC reconstituted with •NO-heme deactivated more rapidly under air compared to nitrogen and the products were oxidized sGC and nitrate (39).

The focus of the work reported here is on the mechanism of deactivation of the •NO-stimulated enzyme. We have expressed rat lung sGC in Sf9 cells using the baculovirus system and purified the recombinant protein to homogeneity. The purified protein contains a stoichiometric equivalent of high-spin ferrous heme. Thorough characterization demonstrated the recombinant protein to be essentially identical to that purified from bovine lung. We found that ferrous-nitrosyl sGC prepared anaerobically and exchanged into aerobic buffer containing no reducing agents was essentially stable on ice and had a half-life of approximately 90 min at 37 °C. Oxyhemoglobin or low molecular weight thiols, such as GSH, greatly accelerated the reversal of •NO-sGC to sGC.

MATERIALS AND METHODS

Unless otherwise specified, all chemicals and reagents were purchased from Sigma. All protein manipulations were carried out at 4 °C, and absorbance spectra were recorded at 10 °C. Buffer pH values were adjusted at 4 °C unless otherwise stated.

Cell Culture. Fall army worm ovary cells (*Spodoptera frugiperda*, Sf9) were grown at 28 °C in monolayer and

suspension cultures in Grace's modified insect medium (Gibco BRL #11605-094) supplemented with 10% fetal calf serum (Hyclone #A-1115-N) and antibiotics (penicillin, streptomycin, and amphotericin B; Sigma #A9909). Monolayer cultures were grown in Costar or Corning tissue culture flasks and suspension cultures in spinner flasks (Bellco Glass Inc.) stirred at 75 rpm. In suspension culture, cells were cultured between 4×10^5 and 3.0×10^6 cells/mL. Cell density and viability were determined by trypan blue exclusion using a hemocytometer.

Infection of Sf9 Cells with Baculoviruses. Recombinant baculoviruses containing the cDNAs for the α - and β -subunits, respectively, of rat lung soluble guanylate cyclase have been described previously (40). High-titer viral stocks were prepared by standard methods. Viral titers were estimated by the limiting dilution method (41). Sf9 cells were coinfecting with the two viruses (MOI = 20 for each virus) at a cell density of 1×10^6 cells/mL in 150 mL suspension cultures by direct addition of high-titer viral stock.

Purification of sGC. Based on protocols previously developed in this laboratory for the purification of sGC from bovine lung (3, 42), the following method was devised. Log-phase Sf9 cells (2.4 L) infected with recombinant baculoviruses were harvested 3 days post-infection by centrifugation, and the pellet was stored at –80 °C. The cell pellet was thawed at 4 °C and resuspended in buffer 1 (25 mM TEA, pH 7.4, 50 mM NaCl, 5 mM DTT, 1 mM EDTA, 1 mM PMSF, 2 mM benzamidin, 1 μ M leupeptin, 1 μ M pepstatin A, 20 mL). Cells were broken by sonication, and particulate material was removed by centrifugation at 200000g for 90 min. The supernatant fraction was applied to a 25 mL (14×1.5 cm) column of Q-Sepharose (Pharmacia) at 0.35 mL/min using a BioRad Econo-system. The column was washed with buffer 1 (50 mL) and developed with a 50–400 mM (100 mL) gradient of NaCl in buffer 1 collecting 2.5 mL fractions. Initially, sGC was identified in fractions by assaying for guanylate cyclase activity. Since the peak of activity coincided exactly with yellow colored fractions eluted by the salt gradient, color was the criterion used to select fractions to be carried through to the next step. Pooled fractions were concentrated to 4 mL in two Ultrafree-15 100K filters (Millipore). The partially purified sGC was applied to a column of Superdex-200 (60×2.6 cm, prepacked, Pharmacia) equilibrated with buffer 2 (25 mM MOPS, pH 7.0, 100 mM NaCl, 5 mM DTT, 1 mM EDTA, 1 mM PMSF, 1 μ M leupeptin, 1 μ M pepstatin A) at a flow rate of 1.4 mL/min using a BioRad BioLogic system. The column was washed with buffer 2 at 1.7 mL/min, collecting 3 mL fractions. Those with an A_{280}/A_{431} ratio <2.5 were pooled and concentrated to 1 mL using an Ultrafree-15 50K filter. The sample was diluted 4-fold with buffer 3 (50 mM MOPS, pH 6.4, 5 mM DTT, 1 mM EDTA, 1 mM PMSF, 1 μ M leupeptin, 1 μ M pepstatin A) and applied to a BioScale S2 column (2 mL, prepacked, BioRad) equilibrated with buffer 4 (25 mM MOPS, pH 6.6, 25 mM NaCl, 5 mM DTT, 1 mM EDTA, 1 mM PMSF, 1 μ M leupeptin, 1 μ M pepstatin A) at a flow rate of 2 mL/min using a BioRad BioLogic system. The column was washed with buffer 4 (6 mL) and developed with a 25–400 mM (20 mL) gradient of NaCl in buffer 4 collecting 1 mL fractions. Those containing pure sGC (as judged by SDS–PAGE) were pooled and concentrated. The final sample was

adjusted to pH 7.4 with 0.5 M MOPS, pH 7.8 and to 0.8 M NaCl with a 4 M solution of NaCl. The protein was either stored overnight under argon for use the following day or mixed with an equal volume of 80% aqueous glycerol and stored under argon at -80°C .

SDS-PAGE. Gel electrophoresis was used to judge purity and to estimate molecular masses of proteins. SDS-PAGE was performed using the Novex minigel system and Novex precast gels as per the manufacturer's instructions. Protein standards were Novex Mark 12 molecular weight markers.

Western Blot. Cross-reactivity of protein bands with anti-bovine lung sGC antisera (Kim and Marletta, unpublished results) was used to identify the α - and β -subunits of sGC in both crude and purified samples of recombinant protein. Western blots were carried out using standard protocols (43) using anti-rabbit IgG-conjugated horseradish peroxidase as the secondary antibody and the ECL chemiluminescent visualization system (Amersham) as per the manufacturer's instructions.

Heme Content and Extinction Coefficient. Protein concentration was determined by the Bradford method using BSA as a standard (Sigma #P-0914) (44). Bradford dye reagent was purchased from BioRad. The assay was calibrated for purified rat lung sGC using quantitative amino acid analysis (QAA). QAA was performed by the University of Michigan Core facility. Briefly, the protein concentration was measured for a sample of sGC by the Bradford method. The sample was then submitted to the Core facility for QAA (performed in triplicate), giving an absolute value for protein concentration. The remaining sample was recovered from the Core facility and the Bradford assay repeated. In each experiment the protein concentration determined by the Bradford assay after QAA agreed with that determined beforehand. This controlled for any potential problems arising through protein precipitation or aggregation which might give an inaccurate correction factor.

The extinction coefficient of the sGC heme Soret (ϵ_{431}) was determined by recording the absorbance spectrum of a sample of sGC, measuring the heme concentration using HPLC, and comparing these values to myoglobin standards. A stock solution of horse heart myoglobin (10 mg/mL, Sigma M1882) was prepared in 20 mM MOPS, pH 7.4, 50 mM NaCl. To measure the heme concentration, the stock solution was diluted 100-fold with 100 mM potassium phosphate, pH 7.4. An aliquot of this solution (400 μL) was placed in a quartz cuvette equipped with a rubber septum and then was deoxygenated using a conventional gas train with seven vacuum/argon cycles with a 1 min equilibration period between each cycle. The sample was reduced by addition of 5 μL of a deoxygenated saturated solution of sodium dithionite using a Hamilton gastight syringe. The heme concentration was calculated using $\epsilon_{434} = 121\,000\text{ M}^{-1}\text{ cm}^{-1}$ (45). The original myoglobin stock was diluted to 0.5–10 μM with 20 mM MOPS, pH 7.4, 50 mM NaCl. Samples of sGC were exchanged into 20 mM MOPS, pH 7.4, 50 mM NaCl using a Pharmacia PD-10 desalting column and concentrated using an Ultrafree-15 50K filter, and the absorbance spectrum was recorded using a Cary 3E spectrophotometer.

Myoglobin standards and sGC samples were analyzed for heme by HPLC using a Waters 600S controller equipped with a 616 pump and 996 photodiode array detector.

Samples were held at 4°C . Samples (50 μL) were applied to a Protein C4 (0.2 μm , 25 cm \times 2.1 mm) column (Vydac) equilibrated with 0.1% aqueous trifluoroacetic acid (TFA) at 0.3 mL/min. The column was developed with a linear gradient of 0.1% aqueous TFA to 0.1% TFA in 30% acetonitrile over 9 mL. Heme was detected at 400 nm, the retention time being 22.3 min with both myoglobin and sGC samples. A standard curve of heme concentration versus peak area was constructed and used to calculate heme concentration in sGC samples (run in triplicate). ϵ_{431} was then calculated from the absorbance spectrum.

Enzyme Activity Assays. Guanylate cyclase activity was measured essentially as described previously (3). Crude or partially purified protein was assayed in 50 mM TEA, pH 7.4, 5 mM MnCl_2 , 2 mM DTT, 0.1 mM GTP, 1 mM IBMX, 5 mM phosphocreatine (PC), and 15 units of creatine kinase (CK) at 37°C in a total volume of 0.1 mL. The reaction was started by addition of enzyme. Sodium nitroprusside was used as a source of $\bullet\text{NO}$ (0.1 mM SNP final concentration). For purified sGC the GTP regenerating system (PC and CK) and phosphodiesterase inhibitor (IBMX) were omitted. The assay mixture contained 50 mM TEA, pH 7.4, 5 mM MgCl_2 , 2 mM DTT, and 1.5 mM GTP. cGMP was quantified using the Amersham radioimmunoassay kit following the supplier's instructions.

Amino Acid Sequencing. N-Terminal amino acid sequences were determined by Edman degradation at the University of Michigan Core facility (Applied Biosystems sequenator). Purified sGC was resolved into separate subunits by SDS-PAGE and the protein transferred to a PVDF membrane by electroblot at 200 mA in 10 mM CAPS, pH 10.5, 0.05% DTT, 10% methanol. The membrane was stained with Coomassie dye to locate the protein bands. The bands were excised, dried in microfuge tubes, and submitted for analysis.

Reversal Experiments. All manipulations were on ice, unless otherwise indicated. The nitrosyl adduct of purified sGC was prepared anaerobically as follows: The sample of sGC was deoxygenated in a 3 mL Teflon-sealed vial or a cuvette equipped with a septum using a conventional gas train with seven vacuum/argon cycles with a 1 min equilibration period between each cycle. A second Teflon-sealed vial (1 mL) was flushed with $\bullet\text{NO}$ (bubbled through a 50% w/v solution of KOH), and a third was flushed with argon. A gastight syringe was flushed with argon from the third vial and used to add a volume of $\bullet\text{NO}$ into the sGC sample. The volume of $\bullet\text{NO}$ used was approximately 1% of the headspace in the reaction vessel. For reversal experiments, the reaction was carried out in a 3 mL Teflon-sealed vial (formation of the $\bullet\text{NO}$ adduct was confirmed by the observation that the protein sample color changed from yellow to pink). The cap was removed, and the sample was exposed to air for 10 min.

A Pharmacia PD-10 desalting column was used to exchange the sample of $\bullet\text{NO}$ -sGC into the buffer required for subsequent manipulations and to remove the excess $\bullet\text{NO}$. The sample volume was adjusted to 0.6 mL with the buffer into which it was to be exchanged and then applied to a Pharmacia PD-10 desalting column equilibrated with the same buffer. The column was washed with 2 mL of buffer and the wash discarded. A further 1.2 mL of buffer was applied, and the eluate (containing the bulk of the protein)

was collected. The nitrosyl-sGC adduct was quantified and verified by recording the absorbance spectrum. In earlier experiments, spectra were recorded using a Cary 3E spectrophotometer. In later experiments, spectra were recorded using a Hewlett-Packard 8453 diode array spectrophotometer. To measure the rate constant for the reversal to the •NO-free species (k_{rev}) at different concentrations of reduced glutathione (GSH), the •NO-sGC adduct was prepared as above and aliquoted such that in each experiment the final volume would be 0.4 mL and the sGC heme concentration 0.5 μM . The buffer used in these experiments was 20 mM MOPS, pH 7.4, 200 mM NaCl; the pH was adjusted at 37 °C. Stock solutions of GSH were prepared in the same buffer to 8 or 80 mM, and the pH was readjusted to 7.4.

For individual experiments, the cuvette was warmed to 37 °C in the instrument. An appropriate volume of GSH stock was added to the •NO adduct on ice such that the final volume was 0.4 mL. This was immediately transferred to the cuvette and data collection initiated. In experiments using the Cary 3E (monochromating) spectrophotometer, spectra were recorded every 3 min over the range 350–701 nm at 675 nm/min with a 1.5 nm data point interval. The diode array spectrophotometer was equipped with a filter opaque to light below 310 nm. Spectra were recorded at 1 nm resolution every 20 or 30 s for 20 or 30 min, respectively, with an acquisition time of 0.2 s for each spectrum. For each spectrum, a buffer base line was subtracted. Absorbances at 399 and 431 nm were extracted and corrected for base line drift by subtracting the average absorbance over the range 695–700 nm. ΔA_{431} and ΔA_{399} were calculated by subtracting the time zero value, and $\Delta\Delta A$ ($\Delta A_{431} - \Delta A_{399}$) calculated for each spectrum. $\Delta\Delta A$ was plotted against time, and the data were fit to a single exponential to yield k_{rev} . For experiments with oxyhemoglobin (HbO₂), •NO-sGC was prepared as above but in 20 mM MOPS, pH 7.4, 50 mM NaCl (adjusted at 37 °C). Buffer plus other reagents were mixed in a separate tube and the sGC sample and reagent sample brought to room temperature. The two were mixed (final volume 0.4 mL, final sGC heme concentration 0.5 μM) and transferred to the cuvette at 37 °C. Data collection was initiated within 5 s of mixing. Human hemoglobin (Sigma H0267) was dissolved in water and the concentration of HbO₂ determined spectrophotometrically. This was aliquoted and stored at –80 °C. Stock solutions of MgCl₂ (200 mM) and Na₃GTP (60 mM) were prepared in 20 mM MOPS, 50 mM NaCl, and the pH was adjusted to 7.4 at room temperature.

RESULTS

Expression of sGC in Insect Cells. Soluble guanylate cyclase was produced by coinfection of *Spodoptera frugiperda* (Sf9) cells with recombinant baculoviruses containing the cDNAs coding for the α - and β -subunits, respectively, of rat lung sGC. The ratio of MOI for the two viruses (1:1) and the total MOI (40) were optimized in monolayer cultures by monitoring guanylate cyclase activity in the 200000g supernatant. A harvest time of 3 days post-infection was found to be optimal in a 150 mL suspension culture. SDS-PAGE of cell lysate 3 days post-infection revealed two new bands in the 70–80 kDa region which reacted with anti-sGC antibody in Western blots (data not shown). Compari-

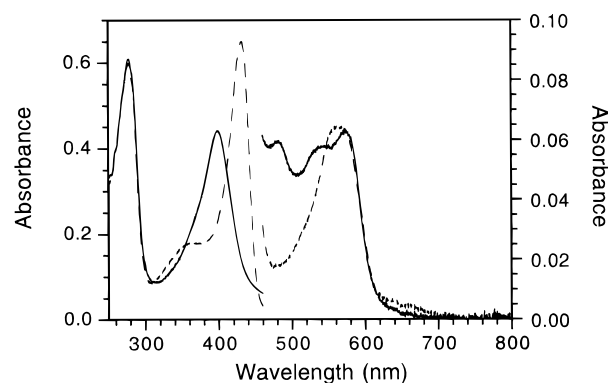


FIGURE 1: Electronic absorption spectra of sGC (0.8 mg/mL) in 20 mM MOPS pH 7.4, 50 mM NaCl at 10 °C under N₂ (dashed line) and under N₂ + 0.5% •NO (solid line). The left scale refers to the Soret region; the right scale refers to the α/β region.

son of cell lysate and 200000g supernatant by SDS-PAGE showed that the bulk of the sGC present was insoluble. The growth temperature was shifted down to 21 or 24 °C immediately post-infection in an attempt to slow protein synthesis and thereby increase the proportion of the recombinant protein remaining soluble. The growth temperature which gave the maximal yield over a 4 day time course was 28 °C.

Purification of sGC from Insect Cells. The purification protocol described under Materials and Methods yielded 0.5–0.7 mg of sGC. SDS-PAGE showed two bands with estimated molecular masses of 82 and 74 kDa, α - and β -subunits, respectively. In some preparations, a third band was visible immediately below the α -subunit band. This band also reacted with anti-sGC antibody (data not shown).

Spectral Studies. The absorbance spectrum of purified recombinant sGC featured a protein absorbance at 278 nm, a δ absorbance centered at 360 nm, a heme Soret absorbance at 431 nm, an α/β absorbance at 565 nm, and a fourth low extinction band at 770 nm (Figure 1). In the presence of •NO, the Soret band shifted to 399 nm, and the α/β band split with new maxima at 542 and 575 nm. A peak was also visible at 482 nm. The low extinction band at 770 nm was not present in this spectrum (Figure 1). The spectral properties of the recombinant protein are essentially identical to those previously purified from bovine lung (3, 4, 42).

Heme Content. Protein concentration was measured by the method of Bradford and by quantitative amino acid analysis. The Bradford:QAA ratio was 0.95 ± 0.1 ($n = 4$); thus, no correction of protein concentration was required when using the Bradford assay. Protein purified from bovine lung by two different methods (S. Kim and M. A. Marletta; J. R. Stone and M. A. Marletta, unpublished results) gave essentially the same result. The extinction coefficient of the heme Soret (ϵ_{431}) was $148\,000 \pm 7000 \text{ M}^{-1} \text{ cm}^{-1}$ ($n = 3$, mean \pm SD). The purified protein contained 0.92 ± 0.1 heme per heterodimer ($n = 7$, mean \pm SD).

Specific Activity. The specific activity of purified sGC was measured with Mg²⁺ as the divalent cation and sodium nitroprusside as a source of •NO. The basal and nitroprusside-stimulated activities were $28 (\pm 7)$ and $18\,700 (\pm 1500) \text{ nmol min}^{-1} \text{ mg}^{-1}$, respectively. Thus, the enzyme was activated 670 (± 220)-fold by •NO. These values are similar to those previously reported by our laboratory given that those activity measurements included a correction factor of

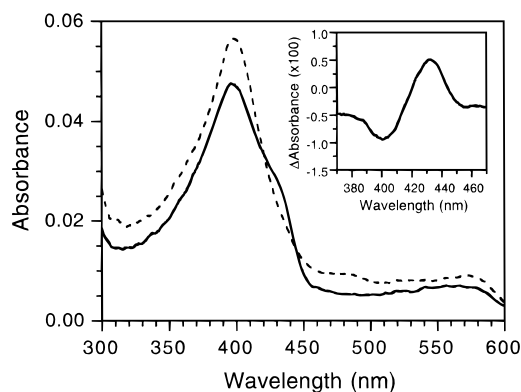


FIGURE 2: Stability of \bullet NO-sGC in aerobic buffer. \bullet NO-sGC was prepared in aerobic 50 mM MOPS, pH 7.4, 5 mM MgCl_2 , 50 mM NaCl as described under Materials and Methods. Spectra shown are immediately after exchange into the above buffer using a PD10 desalting column (dashed line) and the same preparation after 20 h on ice. *Inset*: Difference spectrum, final – initial absorbance spectrum.

1.66 applied to the protein concentrations determined by the Bradford method (42).

N-Terminal Amino Acid Sequences. Subunits of sGC separated by SDS-PAGE were subjected to N-terminal sequencing by Edman degradation. Signals for the two subunits were of approximately equal intensity. The sequence obtained was consistent with that expected from an intact β -subunit, but the first 20 amino acids of the α -subunit were not present (found: APGQVPTEPI). The first residue was not methionine, indicating a posttranslational modification or proteolytic degradation rather than an alternate translation start site or an incomplete cDNA. Previous experiments indicated that the α -subunit of sGC purified from bovine lung was blocked at the N-terminus (18, 46). The cleaved sequence does not bear any significant similarity to known cleavable signal sequences; thus, it is not clear whether the proteolysis observed here is physiologically relevant, or simply an artifact of the expression and purification system.

Reversal from \bullet NO-Bound to \bullet NO-Free sGC. When anaerobically prepared \bullet NO-sGC was exposed to air and exchanged by gel filtration into a buffer containing no reductant (50 mM MOPS, pH 7.4, 5 mM MgCl_2 , 50 mM NaCl), the absorbance spectrum ($\lambda_{\text{max}} = 399$ nm) was identical to the ferrous-nitrosyl sGC spectrum in Figure 1. After 20 h on ice, the absorbance spectrum was unchanged except for a shoulder on the long-wavelength side of the Soret (399 nm) peak (Figure 2). The difference spectrum displayed a maximum at 432 nm and a minimum at 398 nm. This is consistent with the conversion of ferrous-nitrosyl sGC to ferrous sGC. When the sample was warmed to 37 °C, the absorbance spectrum changed over a period of 2 h to one similar to that of ferrous sGC, the Soret maximum having returned to 431 nm (data not shown).

When similarly prepared \bullet NO-sGC was exchanged into the same buffer with DTT (2 mM), a more rapid transition to the ferrous sGC spectrum was observed (Figure 3). The single-exponential rate constant for this spectral shift, k , was 0.16 min^{-1} ($t_{1/2} = 4.2$ min) (Figure 4). In the presence of 0.8 mM L-cysteine, the same transition occurred with $k = 0.12 \text{ min}^{-1}$ ($t_{1/2} = 5.8$ min).

In studying this effect further, the physiological thiol, GSH, was used. The rate at which the spectral transition occurred

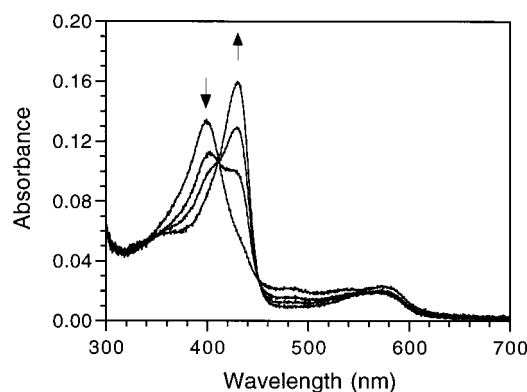


FIGURE 3: Reversal of \bullet NO-sGC to ferrous sGC in the presence of DTT. Ferrous nitrosyl-sGC was prepared in aerobic 50 mM MOPS, pH 7.4, 50 mM NaCl, 5 mM MgCl_2 , 2 mM DTT as described under Materials and Methods. Spectra were recorded during incubation at 37 °C in the spectrophotometer every 3 min at a scan rate of 450 nm/min with a 0.5 nm data interval. The spectra shown are those recorded after 0, 3, 6 and 12 min. The absorbance at 399 nm decreases and the absorbance at 431 nm increases in successive spectra.

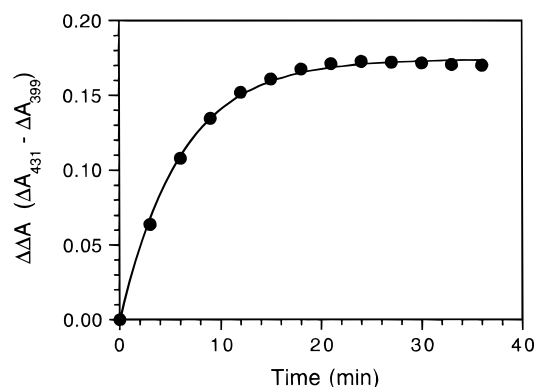


FIGURE 4: Time course of reversal of \bullet NO-sGC to ferrous sGC in the presence of 2 mM DTT. $\Delta\Delta A$ ($\Delta A_{431} - \Delta A_{399}$) was calculated for each spectrum in the experiment depicted in Figure 3 and plotted against time. The total $\Delta\Delta A$ was 0.17. The single-exponential rate constant for the transition was 0.16 min^{-1} ($t_{1/2} = 4.2$ min).

was examined with respect to GSH concentration. Anaerobically prepared \bullet NO-sGC was exchanged into aerobic \bullet NO-free buffer (20 mM MOPS, pH 7.4, 200 mM NaCl) by gel filtration. GSH was added at varying concentrations, and the rate constant for reversal to the ferrous sGC spectrum (k_{rev}) was determined as described under Materials and Methods (Figure 5). For example, when GSH was present at 1 mM, the value determined for k_{rev} was 0.11 min^{-1} ($t_{1/2} = 6.3$ min). In the absence of GSH, the transition was slow and was approximately linear over the time measured. The $t_{1/2}$ for this transition was estimated to be 90 min, giving a value for k_{rev} of approximately 0.008 min^{-1} . The dependence of k_{rev} on GSH concentration has two distinct phases (Figure 6). At low concentrations of GSH (0.1–4 mM), a saturable increase in k_{rev} occurred. At higher concentrations of GSH (4–24 mM), a linear dependence of k_{rev} on GSH concentration was apparent.

Previous studies of the formation of S-nitrosoglutathione (GSNO) from GSH and \bullet NO in aerobic solution and of the release of \bullet NO from GSNO in aerobic solution indicated that contaminating transition metal ions (copper and iron) present in buffer solutions could catalyze the respective processes (47–49). In each case the effect of metal ions

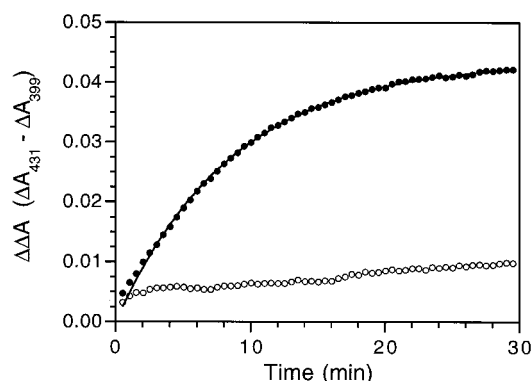


FIGURE 5: Time course of reversal of •NO-sGC to ferrous sGC in the presence of GSH. Ferrous nitrosyl-sGC was prepared in aerobic 20 mM MOPS, pH 7.4, 200 mM NaCl as described under Materials and Methods. Spectra were recorded every 30 s, and $\Delta\Delta A$ ($\Delta A_{431} - \Delta A_{399}$) was calculated as described under Materials and Methods in the absence (open circles) or presence (filled circles) of 1 mM GSH. For the GSH experiment, data fit to a single exponential gave an observed rate constant, k_{rev} , of 0.11 min^{-1} .

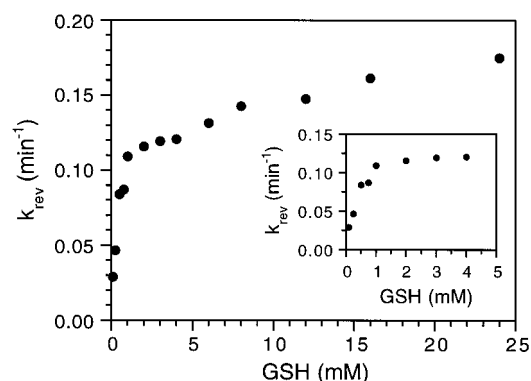


FIGURE 6: Dependence of the observed rate constant for reversal of •NO-sGC to ferrous sGC on GSH concentration. The experiment depicted in Figure 5 was conducted for various concentrations of GSH and the observed rate constant for reversal of •NO-sGC to ferrous sGC determined for each concentration of GSH. The inset is an expansion of the GSH concentration range 0.1–4 mM.

Table 1: Summary of Rates of Reversal of •NO-sGC to Ferrous sGC^a

additions	rate constant (min^{-1})	half-life (min)
2 mM DTT ¹	0.16	4.3
0.8 mM L-Cys ¹	0.12	5.8
none ²	0.008	86.6
1 mM GSH ²	0.11	6.3
1 mM GSH, 0.5 mM EDTA ²	0.08	8.7
1 mM GSH, 0.1 mM cGMP ²	0.09	7.7
2 μM HbO ₂ ³	0.28	2.5
2 μM HbO ₂ , 1 mM GSH ³	0.24	2.9
2 μM HbO ₂ , 1 mM GSH, MgGTP ³	0.22	3.1

^a Rate constants were determined as described under Materials and Methods. Buffer constituents were ¹50 mM MOPS, pH 7.4, 50 mM NaCl, 5 mM MgCl₂, ²20 mM MOPS, pH 7.4, 200 mM NaCl, or ³20 mM MOPS, pH 7.4, 50 mM NaCl.

was negated by the addition of EDTA. Inclusion of 0.5 mM EDTA in reversal experiments did not prevent acceleration of the rate of reversal by 1 mM GSH (see Table 1).

A recent report of effects of GTP on •NO bound to sGC using resonance Raman spectroscopy suggested that cGMP may regulate the activity of sGC by controlling the binding

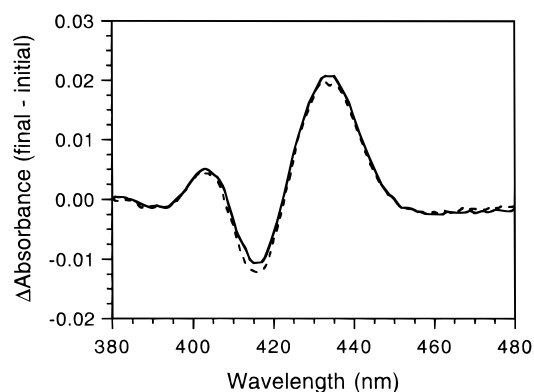


FIGURE 7: Difference spectra of reversal of •NO-sGC to ferrous sGC in the absence (solid line) and presence (dashed line) of MgGTP. Ferrous-nitrosyl sGC was prepared in 20 mM MOPS, pH 7.4, 50 mM NaCl as described under Materials and Methods. Incubations contained 0.5 μM sGC heme, 2 μM HbO₂, 1 mM GSH, with or without substrate (3 mM Na₃GTP, 5 mM MgCl₂) and were carried out at 37 °C. Data were collected for 30 min (interval 15 s).

of •NO to sGC (50). Addition of cGMP to 100 μM in the presence of 1 mM GSH did not significantly change k_{rev} compared to that with 1 mM GSH alone.

A recent report by Kharitonov et al. provided evidence that the deactivation of soluble guanylate cyclase was greatly accelerated in the presence of substrate (MgGTP) (38). Specifically, these workers used oxymyoglobin (MbO₂) to trap unbound •NO and monitored the increase in absorbance at 435 nm (i.e., regeneration of ferrous high-spin sGC-heme). Since that observation bears directly on the results reported here, we sought to reproduce that experiment and investigate the effect of GSH in that system. •NO-sGC was prepared anaerobically and exchanged into aerobic •NO-free 20 mM MOPS, pH 7.4, 50 mM NaCl as described under Materials and Methods. These experiments had to be performed under known turnover conditions to be valid. Therefore, a lower NaCl concentration was used than in previous reversal experiments with GSH since higher salt concentrations inhibit sGC activity (S. Kim and M. A. Marletta, unpublished results). Incubation of •NO-sGC at 37 °C in the presence of oxyhemoglobin (HbO₂, 2 μM) and GSH (1 mM) resulted in a time-dependent change in the absorbance spectrum with increases centered at 405 and 434 nm, and a decrease centered at 416 nm (Figure 7). When •NO-sGC was similarly incubated with GSH (1 mM), but no HbO₂, a time-dependent reversal to the ferrous form ($\lambda_{\text{max}} = 431 \text{ nm}$) was observed as with DTT. The isosbestic point was at 415 nm. Thus, we can reasonably assign the peaks in the difference spectrum in Figure 7 as follows: 434 nm, appearance of ferrous sGC heme; 416 nm, disappearance of HbO₂; 405 nm, a combination of disappearance of •NO-sGC and appearance of methemoglobin. The rate constant for the increase in absorbance at 434 nm ($k\Delta A_{434}$) was 0.24 min^{-1} . Under these conditions, inclusion of substrate, MgGTP (3 mM Na₃GTP, 5 mM MgCl₂), had no significant effect on the observed spectral transitions (Figures 7 and 8). In the presence of substrate, $k\Delta A_{434}$ was 0.22 min^{-1} . Comparable experiments carried out at 20 °C over time-courses of 60 s also showed

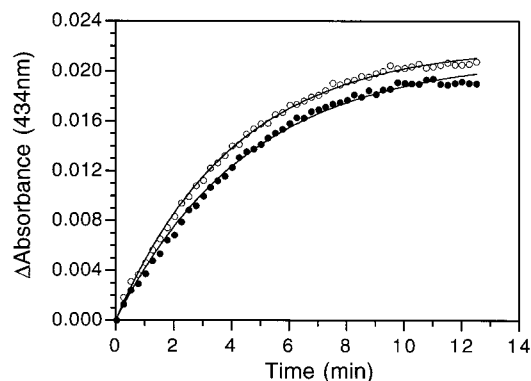


FIGURE 8: Reversal of \bullet NO-sGC to ferrous sGC in the absence (open circles) and presence (filled circles) of MgGTP. The change in absorbance at 434 nm in the experiment described in Figure 7 was plotted against time. Ferrous-nitrosyl sGC was prepared in 20 mM Mops, pH 7.4, 50 mM NaCl as described under Materials and Methods. Incubations contained 0.5 μ M sGC heme, 2 μ M HbO₂, 1 mM GSH, \pm substrate (3 mM Na₃GTP, 5 mM MgCl₂), and were carried out at 37 °C. Data were collected for 30 min (interval 15 s), and ΔA (434 nm) was fit to a single exponential. k_{rev} for the transition in the absence of substrate was 0.24 min⁻¹ ($t_{1/2}$ = 2.9 min); k_{rev} for the transition in the presence of substrate was 0.22 min⁻¹ ($t_{1/2}$ = 3.2 min).

no difference in the absence or presence of substrate (data not shown). To verify that the concentration of HbO₂ used in the experiments conducted at 37 °C was not limiting, the HbO₂ concentration was varied from 0.5 to 4 μ M. The time course of reversal was the same in each case (data not shown). We attempted to examine the reversal process in the presence of substrate and in the absence of GSH or HbO₂, but these experiments were hampered by the appearance of a precipitate in the incubation mixture. This precipitate did not appear in the absence of substrate (MgGTP) and did not appear in the presence of substrate when sGC was rapidly deactivated (as inferred from the spectral transition to the \bullet NO-free, ferrous sGC). In the absence of substrate, acceleration of reversal by HbO₂ was not dependent on the presence of GSH. Also, the rate of reversal in the presence of HbO₂ was not increased by the addition of GSH. Rates of reversal are summarized in Table 1.

DISCUSSION

Expression, Purification, and Characterization of Recombinant sGC. The expression and purification system reported here gives the highest yield of heme-containing soluble guanylate cyclase (sGC) purified from a recombinant source to date. Also, this is the first report detailing a preparation of sGC with a stoichiometric equivalent of bound heme. Correspondingly, the fold-activation by nitric oxide is the highest yet reported. Activation of catalytic activity by \bullet NO has been shown to correlate with heme content (42). Previously described recombinant systems include several examples of transient expression in mammalian cell lines (16, 51, 52). These systems have primarily been used for initial characterizations of sGC isoforms and mutants. Some of the previous reports have employed an insect cell/baculovirus system similar to the one reported here (51–53).

Previous results reported by our laboratory indicated a native heme stoichiometry of 2 per heterodimer (42); however, the experiments reported here conclusively show

that the native stoichiometry is 1 heme per heterodimer. Experiments in our laboratory directed toward resolving this apparent contradiction suggested that the method of preparation of protein for quantitative amino acid analysis used to calibrate the Bradford protein assay was the source of error. Furthermore, the heme binding site has been localized to the N-terminal 385 amino acid residues of the β -subunit and the axial ligand identified as histidine- β 105 by a combination of site-directed mutagenesis, UV–visible spectroscopy, and resonance Raman spectroscopy (23, 52, 54). In short, native sGC contains one heme per heterodimer, the heme is localized in the smaller, β -subunit, and the axial ligand is histidine-105.

When Tomita et al. purified sGC from bovine lung, they determined the heme content of that preparation to be 0.8 heme/dimer using the pyridine–hemochromagen assay for heme and the Bradford assay for protein (50). The data presented here are consistent with that finding, except that our data gave a larger value (148 000 M⁻¹ cm⁻¹) for the Soret extinction coefficient (ϵ_{431}) than the value of approximately 90 000 M⁻¹ cm⁻¹ calculated from Figure 1 in (50). It is not clear why two very different extinction coefficients should be measured from what are otherwise very similar protein samples.

Based on the spectral characterization, the heme environment of the recombinant protein is identical to heterodimeric sGC purified from tissue. The specific activity of the recombinant material was comparable to that of sGC from tissue, indicating that the catalytic site is correctly formed. Catalysis was activated 670-fold by \bullet NO (from nitroprusside), confirming that communication between the heme site and the catalytic site is also functional. Thus, results obtained with this recombinant sGC will most likely also be true for sGC present in tissue.

Deactivation of sGC in Vivo. The mechanism of activation of sGC by \bullet NO continues to be an important question in our understanding of the \bullet NO-signaling pathway. Of equal importance is the mechanism of deactivation of sGC. Deactivation is known to be a tightly regulated process in the context of blood pressure control. Palmer et al. showed that tissue which relaxed in response to \bullet NO-mediated stimulus rapidly contracted back to its original state, with the half-time being 1–2 min (33). The same preparation could be stimulated to relax by a second \bullet NO-mediated stimulus directly after the first, indicating that the signaling system was deactivated by \bullet NO dissociating from sGC. The half-lives for dissociation of \bullet NO from typical nitrosyl complexes of hemoproteins such as myoglobin and T- and R-state hemoglobin are variable, ranging from 11.5 min to 10.7 h at 20 °C (34–36). Resonance Raman and FTIR spectroscopic data suggested that negative polarity in the distal side of the sGC heme pocket might be a potential mechanism by which the dissociation rate for \bullet NO could be increased compared with other hemoproteins (22, 55). Nonprotein studies found that dissociation of \bullet NO from heme model compounds (5-coordinate ferrous-nitrosyl complexes) varied by 6 orders of magnitude depending on the porphyrin structure and the competing ligand (37). Therefore, the question we sought to address was whether simple dissociation of \bullet NO from sGC can account for the observed rate of deactivation in vivo.

Dissociation Versus Oxidation. Before addressing the problem of the rate of deactivation of sGC, we must first determine whether deactivation in the presence of oxygen occurs via loss of •NO to regenerate ferrous-sGC or whether ferrous-nitrosyl sGC is oxidized to ferric sGC and nitrate. Dierks and Burstyn have presented data which indicate that •NO-sGC, in aerobic solution, is slowly oxidized to ferric sGC and nitrate as is the case with •NO-hemoglobin and •NO-myoglobin (39). Nitrate was identified as the major nitrogen oxide product, and the appearance of low-spin ferric sGC ($\lambda_{\text{max}} = 420 \text{ nm}$) was followed spectrally. We found that the ferrous nitrosyl-sGC complex was relatively stable in aerobic buffer in the absence of any reductant. Analysis of the spectra immediately after preparation of the •NO-sGC adduct and after 20 h on ice indicated that decomposition of •NO-sGC did not result in oxidation of the heme group. The most likely explanation is that •NO was the species dissociating from sGC heme. This observation is consistent with the low affinity of sGC for O₂ as described above; i.e., following dissociation of •NO, sGC did not bind O₂ and then react with •NO to give ferric sGC and nitrate as is likely the case with Hb and Mb. The protein preparation used in this study was isolated with a stoichiometric equivalent of heme, whereas Dierks and Burstyn used sGC reconstituted with •NO-heme after purification. The difference in behavior of the two preparations suggests that the heme is in different environments in the two cases. This in turn suggests that reconstitution of sGC with •NO-heme does not result in a native heme environment, even though the reconstituted complex displays a specific activity one-quarter of that reported here.

Stability of Ferrous-Nitrosyl sGC. This apparent stability of •NO-sGC could be explained by the fact that at low concentrations •NO is quite stable in aerobic buffer since the kinetics of reaction of •NO with O₂ are second order with respect to •NO concentration (56, 57). For example, the first half-life of 100 nM •NO at 25 °C in the presence of 100 μM oxygen would be approximately 21 min (46). Thus, when •NO-sGC was prepared in aerobic, •NO- and thiol-(reductant) free buffer, an equilibrium was established between •NO bound to sGC and a low but persistent concentration of •NO (eq 1). There was no discernible difference between the absorbance spectrum of anaerobic •NO-sGC and that after aerobic buffer exchange. This would imply that the equilibrium must lie predominantly to the left.



The in vitro stability of •NO-sGC is not consistent with the rapid in vivo deactivation indicated by the work of Palmer et al. as described above. There are three credible mechanisms by which reversal could be accelerated in vivo. First, unbound •NO is efficiently trapped in vivo (e.g., by other hemoproteins), preventing rebinding of •NO after dissociation. Second, some compound in the cell reacts directly with •NO-sGC to remove •NO. Third, some regulatory event increases k_{off} , leading to rapid deactivation. We sought to investigate these possibilities.

Acceleration of Reversal by Thiols. We found that inclusion of DTT or other thiol reagents such as GSH or L-cysteine increased the rate at which the reversal to the original ferrous sGC spectrum occurred. We hypothesized

that this was because the thiol was accelerating the decomposition of free •NO, thus drawing the equilibrium in eq 1 to the right. However, Gow et al. found that when cysteine (0.75 mM) was added to an 0.75 μM aerobic solution of •NO at 22 °C, the rate of •NO loss as measured using an •NO-specific electrode was approximately 3.8 nM/s compared to approximately 1.6 nM/s in the absence of cysteine (58). This is only a 2.4-fold increase in loss of •NO in the presence of thiol. Our results demonstrated that an increase in the rate of reversal of •NO-sGC to ferrous sGC in the presence of 0.8 mM L-cysteine was approximately 15-fold over that in the absence of thiol. The difference between Gow's observation and ours might have been explained by the presence of trace amounts of transition metals in our buffers which have been shown to catalyze the reaction of •NO with cysteine in aerobic solution (49). However, at least with GSH, we found that the rate increase was likely not due to metal catalysis since EDTA did not inhibit the effect. It should be noted that the experimental method employed here measures the disappearance of •NO-sGC and the appearance of ferrous sGC and is independent of the mechanism of destruction of •NO.

Thus, it was unclear why thiols should have such an effect on the reversal to ferrous sGC. Therefore, the next step was to examine the dependence of the rate of reversal on thiol concentration. Since GSH is the predominant physiological low molecular weight cytosolic thiol, it was used for these experiments. GSH is present in tissue at millimolar concentrations (59). Accordingly, k_{rev} was determined in the presence of GSH over the range 0.1–24 mM. The dependence of k_{rev} on GSH concentration was biphasic, suggesting that GSH accelerates the loss of •NO to re-form ferrous sGC by two different mechanisms. The first mechanism predominates at high micromolar concentrations of GSH (100–750 μM), above which the rate of reversal becomes independent of GSH concentration indicating that free GSH is not a reactant species in the rate-determining step. A second mechanism then predominates at millimolar concentrations of GSH which exhibits a linear dependence on GSH concentration. It is tempting to assign this phase to oxygen-dependent, metal-independent reaction of •NO with GSH to give S-nitrosoglutathione (GSNO) and/or oxidized glutathione (GSSG). In the same vein, GSH can increase the concentration of superoxide anion in the system via a one-electron reduction of oxygen. Superoxide reacts with •NO to form peroxynitrite. If this was the dominant mechanism of destruction of •NO in the present system, then superoxide dismutase would be expected to inhibit the reversal to ferrous sGC. This was not the case (data not shown). The involvement of oxygen will be tested further by examining the effect of GSH on •NO-sGC under anaerobic conditions.

The saturable dependence of k_{rev} on GSH concentration implies that GSH forms some reversible complex with another component of the system and that reaction of that species is rate-limiting. Since the method employed in this work measures the disappearance of •NO-sGC and the appearance of ferrous sGC, and is independent of the route by which •NO is lost from the system, this saturable behavior would not be observed if •NO were irreversibly lost by oxidation to N₂O₃ which in turn reacted with GSH. Decomposition of •NO in aerobic aqueous solution by this route has been studied in detail by Kharitonov et al. (49). Also,

the saturation effect at lower concentrations of GSH cannot be explained by the notion that actual dissociation of $\bullet\text{NO}$ from sGC becomes rate-limiting since at higher GSH concentrations a further increase in k_{rev} was observed. One explanation might be that GSH forms a reversible complex with sGC itself and subsequently accelerates dissociation of $\bullet\text{NO}$. Whether such a complex would be a Michaelis type adduct in which GSH reacts with protein-bound $\bullet\text{NO}$ or a covalently linked species, through a protein thiol, for example, is purely speculative. It has long been known that protein thiols play a role in the catalytic activity and regulation of sGC. Treatment of sGC with thiol-modifying reagents led to loss of activity which could be reversed with reducing thiols (DTT, GSH) or which was blocked by substrate (60, 61). Zwiller et al. found that partially purified sGC bound to thiol-Sepharose and could be eluted with cysteine, indicating the presence of an exposed thiol (62). These conclusions were corroborated by a model of the sGC catalytic domain (based on homology with the adenylate cyclase catalytic core) which placed a free thiol in the substrate binding site (63). Also recently, Friebe et al. have demonstrated a role for sGC cysteine residues in heme binding, although it is not known if those same residues play a role in the activation/deactivation process (51). Experiments are in progress in our laboratory to identify free thiols in the heme site of sGC.

Acceleration of Reversal by Oxyhemoglobin. When HbO_2 was used to trap $\bullet\text{NO}$, we observed an increase in the rate of reversal compared to when $\bullet\text{NO}$ -sGC was incubated in buffer alone. The concentration of HbO_2 was not rate-limiting at 2 μM (a 4-fold excess over $\bullet\text{NO}$ -sGC). The obvious explanation for this is that inclusion of the trap prevents rebinding of $\bullet\text{NO}$ to sGC following simple dissociation. It is interesting to note that the rates of loss of $\bullet\text{NO}$ in the presence of HbO_2 , 0.22–0.28 min^{-1} at 37 $^\circ\text{C}$ (this study) and 0.033 min^{-1} at 20 $^\circ\text{C}$ (36), are faster than expected from studies by Kharitonov et al. with 5-coordinate heme-nitrosyl model compounds and 5-coordinate human serum albumin-heme-NO complexes (36). In fact, that study showed that only T-state $\bullet\text{NO}$ -Hb displayed a faster $\bullet\text{NO}$ off-rate than $\bullet\text{NO}$ -sGC. Thus, sGC has evolved such that the unique environment of the heme group bound to the protein allows sGC to reversibly bind $\bullet\text{NO}$ consistent with its role as an $\bullet\text{NO}$ -sensor. Contrary to the published results of Kharitonov et al. (38), addition of substrate (GTP/ Mg^{2+}) to $\bullet\text{NO}$ -sGC in the presence of GSH and HbO_2 did not affect the rate of reversal. We are currently trying to rationalize these observations by studying the effect of a nonhydrolyzable analogue of GTP, thus removing the complicating issue of turnover to products. Thus, both glutathione and oxyhemoglobin can accelerate the reversal of ferrous-nitrosyl sGC to ferrous sGC. The upper limits of the associated rate constants are close in value (0.18 and 0.24 min^{-1} , respectively), but neither is fast enough to account for deactivation in vivo.

Summary. Of the three potential mechanisms for rapid deactivation of sGC in vivo that were presented above, the first, prevention of rebinding of $\bullet\text{NO}$ to sGC by hemoproteins, could account for part of the difference in the rate of deactivation of sGC in vitro versus in vivo. It seems that low molecular weight thiols such as GSH could contribute to this. The second of the three, the notion that some

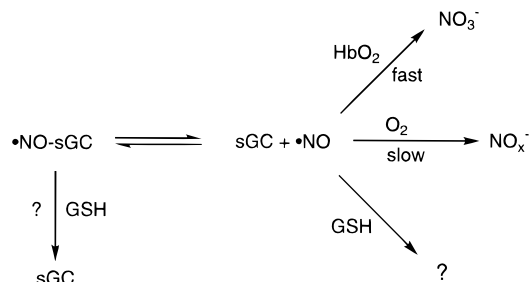


FIGURE 9: Potential in vivo deactivation mechanisms of sGC. Deactivation of the enzyme could occur by prevention of $\bullet\text{NO}$ rebinding to the enzyme. Three possible reactions are shown. The direct solution reaction of $\bullet\text{NO}$ with GSH would require the participation of an electron acceptor, e.g., a metal ion. Alternatively, reaction of $\bullet\text{NO}$ -sGC directly with thiols such as GSH could lead to deactivated enzyme.

compound in the cell reacts directly with $\bullet\text{NO}$ -sGC to remove $\bullet\text{NO}$, may also operate; i.e., GSH may interact directly with $\bullet\text{NO}$ -sGC. These possibilities are summarized in Figure 9. The third mechanism was an increase in k_{off} brought about by allosteric regulation of sGC. At present, we have no evidence for such a mechanism, although further investigation into allosteric regulation of sGC is underway in our laboratory.

Thus, after considering the results presented here, it seems that factors other than thiol- and oxygen-dependent loss of $\bullet\text{NO}$ and trapping by hemoproteins may also influence the rate of deactivation of soluble guanylate cyclase in vivo. What these factors are remains to be determined.

ACKNOWLEDGMENT

We acknowledge members of the Marletta laboratory for useful discussion and critical evaluation of the manuscript, Dr. Yoichi Osawa for HPLC, and Drs. James R. Stone and Seonyoung Kim for sGC purified from bovine lung and anti-sGC antisera (S.K.).

REFERENCES

- Waldman, S. A., and Murad, F. (1987) *Pharmacol. Rev.* 39, 163–196.
- Schmidt, H. H. W., Lohmann, S. M., and Walter, U. (1993) *Biochim. Biophys. Acta* 1178, 153–175.
- Stone, J. R., and Marletta, M. A. (1994) *Biochemistry* 33, 5636–5640.
- Stone, J. R., Sands, R. H., Dunham, W. R., and Marletta, M. A. (1995) *Biochem. Biophys. Res. Commun.* 207, 572–577.
- Gerzer, R., Böhme, E., Hofmann, F., and Schultz, G. (1981) *FEBS Lett.* 132, 71–74.
- Marletta, M. A. (1994) *Cell* 78, 927–930.
- Garbers, D. L. (1992) *Cell* 71, 1–4.
- Yuen, P. S. T., and Garbers, D. L. (1992) *Annu. Rev. Neurosci.* 15, 193–225.
- Garbers, D. L., and Lowe, D. G. (1994) *J. Biol. Chem.* 269, 30741–30744.
- Taussig, R., and Gilman, A. G. (1995) *J. Biol. Chem.* 270, 1–4.
- Chinkers, M., Garbers, D. L., Chang, M.-S., Lowe, D. G., Chin, H., Goeddel, D. V., and Schulz, S. (1989) *Nature* 338, 78–83.
- Dessauer, C. W., Scully, T. T., and Gilman, A. G. (1997) *J. Biol. Chem.* 272, 22272–22277.
- Thompson, D. K., and Garbers, D. L. (1995) *J. Biol. Chem.* 270, 425–430.
- Garbers, D. L. (1979) *J. Biol. Chem.* 254, 240–243.

15. Kamisaki, Y., Saheki, S., Nakane, M., Palmieri, J. A., Kuno, T., Chang, B. Y., Waldman, S. A., and Murad, F. (1986) *J. Biol. Chem.* 261, 7236–7241.
16. Nakane, M., Arai, K., Saheki, S., Kuno, T., Buechler, W., and Murad, F. (1990) *J. Biol. Chem.* 265, 16841–16845.
17. Koesling, D., Herz, J., Gausepohl, H., Niroomand, F., Hinsch, K.-D., Mulsch, A., Bohme, E., Schultz, G., and Frank, R. (1988) *FEBS Lett.* 239, 29–34.
18. Koesling, D., Harteneck, C., Humbert, P., Bosserhoff, A., Frank, R., Schultz, G., and Bohme, E. (1990) *FEBS Lett.* 266, 128–132.
19. Giuili, G., Scholl, U., Bulle, F., and Guellaen, G. (1992) *FEBS Lett.* 304, 83–88.
20. Shah, S., and Hyde, D. R. (1995) *J. Biol. Chem.* 270, 15368–15376.
21. Mikami, T., Kusakabe, T., and Suzuki, N. (1998) *Eur. J. Biochem.* 253, 42–48.
22. Deinum, G., Stone, J. R., Babcock, G. T., and Marletta, M. A. (1996) *Biochemistry* 35, 1540–1547.
23. Zhao, Y., Schelvis, J. P. M., Babcock, G. T., and Marletta, M. A. (1998) *Biochemistry* 37, 4502–4509.
24. Doyle, M. P., and Hoekstra, J. W. (1981) *J. Inorg. Biochem.* 14, 351–358.
25. Eich, R. F., Li, T., Lemon, D. D., Doherty, D. H., Curry, S. R., Aitken, J. F., Mathews, A. J., Johnson, K. A., Smith, R. D., Phillips, G. N., and Olson, J. S. (1996) *Biochemistry* 35, 6976–6983.
26. Dierks, E. A., Hu, S., Vogel, K. M., Yu, A. E., Spiro, T. G., and Burstyn, J. N. (1997) *J. Am. Chem. Soc.* 119, 7316–7323.
27. Stone, J. R., and Marletta, M. A. (1996) *Biochemistry* 35, 1093–1099.
28. Ko, F. N., Wu, C. C., Kuo, S. C., Lee, F. Y., and Teng, C. M. (1994) *Blood* 84, 4226–4233.
29. Friebe, A., Schultz, G., and Koesling, D. (1996) *EMBO J.* 15, 6863–6868.
30. Mulsch, A., Bauersachs, J., Schafer, A., Stasch, J.-P., Kast, R., and Busse, R. (1997) *Br. J. Pharmacol.* 120, 681–689.
31. Stone, J. R., and Marletta, M. A. (1998) *Chem. Biol.* 5, 255–261.
32. Zhang, G., Liu, Y., Ruoho, A. E., and Hurley, J. H. (1997) *Nature* 386, 247–253.
33. Palmer, R. M. J., Ferrige, A. G., and Moncada, S. (1987) *Nature* 327, 524–526.
34. Cassoly, R., and Gibson, Q. H. (1975) *J. Mol. Biol.* 91, 301–313.
35. Sharma, V. S., and Ranney, H. M. (1978) *J. Biol. Chem.* 253, 6467–6472.
36. Kharitonov, V. G., Sharma, V. S., Magde, D., and Koesling, D. (1997) *Biochemistry* 36, 6814–6818.
37. Bohle, D. S., and Hung, C. H. (1995) *J. Am. Chem. Soc.* 117, 9584–9585.
38. Kharitonov, V. G., Russwurm, M., Magde, D., Sharma, V. S., and Koesling, D. (1997) *Biochem. Biophys. Res. Commun.* 239, 284–286.
39. Dierks, E. A., and Burstyn, J. N. (1998) *Arch. Biochem. Biophys.* 351, 1–7.
40. Buechler, W., Singh, S., Aktas, J., Muller, S., Murad, F., and Gerzer, R. (1995) *Adv. Pharmacol.* 34, 293–303.
41. O'Reilly, D. R., Miller, L. K., and Luckow, V. A. (1994) *Baculovirus Expression Vectors*, Oxford University Press, New York.
42. Stone, J. R., and Marletta, M. A. (1995) *Biochemistry* 34, 14668–14674.
43. Ausubel, F. M., Brent, R., Kingston, R. E., Moore, D. D., Smith, J. A., Seidman, J. G., and Struhl, K. (1995) *Current Protocols in Molecular Biology*, John Wiley & Sons, Inc., New York.
44. Bradford, M. M. (1976) *Anal. Biochem.* 72, 248–254.
45. Antonini, E., and Brunori, M. (1971) *Hemoglobin and myoglobin in their reactions with ligands*, North-Holland Publishing Co., Amsterdam.
46. Stone, J. R. (1995) Ph.D. Dissertation, University of Michigan, Ann Arbor, MI.
47. McAninly, J., Williams, D. L. H., Askew, S. C., Butler, A. R., and Russell, C. (1993) *J. Chem. Soc., Chem. Commun.*, 1758–1759.
48. Askew, S. C., Barnett, D. J., McAninly, J., and Williams, D. L. H. (1995) *J. Chem. Soc., Perkin Trans. 2*, 741–745.
49. Kharitonov, V. G., Sundquist, A. R., and Sharma, V. S. (1995) *J. Biol. Chem.* 270, 28158–28164.
50. Tomita, T., Ogura, T., Tsuyama, S., Imai, Y., and Kitigawa, T. (1997) *Biochemistry* 36, 10155–10160.
51. Friebe, A., Wedel, B., Harteneck, C., Foerster, J., Schultz, G., and Koesling, D. (1997) *Biochemistry* 36, 1194–1198.
52. Wedel, B., Humbert, P., Harteneck, C., Foerster, J., Malkewitz, J., Bohme, E., Schultz, G., and Koesling, D. (1994) *Proc. Natl. Acad. Sci. U.S.A.* 91, 2592–2596.
53. Wedel, B., Harteneck, C., Foerster, J., Friebe, A., Schultz, G., and Koesling, D. (1995) *J. Biol. Chem.* 270, 24871–24875.
54. Zhao, Y., and Marletta, M. A. (1997) *Biochemistry* 36, 15959–15964.
55. Kim, S., Deinum, G., Gardner, M. T., Marletta, M. A., and Babcock, G. T. (1996) *J. Am. Chem. Soc.* 118, 8769–8770.
56. Ford, P. C., Wink, D. A., and Stanbury, D. M. (1993) *FEBS Lett.* 326, 1–3.
57. Goldstein, S., and Czapski, G. (1995) *J. Am. Chem. Soc.* 117, 12078–12084.
58. Gow, A. J., Buerk, D. G., and Ischiropoulos, H. (1997) *J. Biol. Chem.* 272, 2841–2845.
59. Meister, A., and Anderson, M. E. (1983) *Annu. Rev. Biochem.* 52, 711–760.
60. Kamisaki, Y., Waldman, S. A., and Murad, F. (1986) *Arch. Biochem. Biophys.* 251, 709–714.
61. Brandwein, H. J., Lewicki, J. A., and Murad, F. (1981) *J. Biol. Chem.* 256, 2958–2962.
62. Zwiller, J., Basset, P., and Mandel, P. (1981) *Biochim. Biophys. Acta* 658, 64–75.
63. Liu, Y., Ruoho, A. E., Rao, V. D., and Hurley, J. H. (1997) *Proc. Natl. Acad. Sci. U.S.A.* 94, 13414–13419.

BI9814989